Analysis of a photon assisted field emission device

K. L. Jensen,[a] Y. Y. Lau,[b] and D. S. McGregor[b]
Code 6841, Electronic Science and Technology Division, Naval Research Laboratory, Washington, DC 20375-5347

(Received 10 February 2000; accepted for publication 27 May 2000)

A field emitter array held at the threshold of emission by a dc gate potential from which current pulses are triggered by the application of a laser pulse on the backside of the semiconductor may produce electron bunches (''density modulation'') at gigahertz frequencies. We develop an analytical model of such optically controlled emission from a silicon tip using a modified Wentzel–Kramers–Brillouin and Airy function approach to solving Schrödinger's equation. Band bending and an approximation to the exchange-correlation effects on the image charge potential are included for an array of hyperbolic emitters with a distribution in tip radii and work function. For a simple relationship between the incident photon flux and the resultant electron density at the emission site, an estimation of the tunneling current is made. An example of the operation and design of such a photon-assisted field emission device is given. © *2000 American Institute of Physics.* [S0003-6951(00)00730-0]

In comparison to solid state devices, microwave power tubes provide higher power operation with larger currents, higher threshold for voltage breakdown, and increased bandwidth due to the higher electron mobility in vacuum.[1] Field emitter arrays (FEAs) offer opportunities for advanced amplifiers by virtue of high current density and high pulse repetition frequencies.[2] Dramatic improvements in amplifier performance are enabled by density modulation.[3] In particular, bunching the electron beam at the cathode surface would eliminate a substantial portion of the interaction circuit, enabling reductions in overall dimensions and weight, through the elimination of the premodulation circuit. A study by Whaley *et al.*[4] concluded that a FEA traveling wave tube (TWT) will have attractive performance capabilities not achievable with a conventional thermionic TWT.

Density modulation carries a cost. Premature FEA failure due to arcing at current levels two orders of magnitude smaller than design requirements precluded success for a program to incorporate FEAs into a power tube.[5] Because of the high-frequency (10 GHz) modulation of the gate potential and the inherent FEA capacitance, resistive protection of the FEA ring cathodes was not available. Hence, the individual emitters were driven hard and were not protected against arc damage. We shall discuss an alternate method for producing electron bunches by optical means. A fundamental description of the emission mechanism from a semiconductor surface is given, including band bending and exchange-correlation effects, leading to a qualitative estimation of array performance, and an assessment of impact on device performance.

If a semiconductor field emitter array is held at the threshold of emission by a dc gate potential, current pulses can be generated by the application of a laser pulse on the backside of the semiconductor—in contrast to previous literature which treat illumination of an emitter tip, or laser generated electron bunches, by front-side illumination.[6] Density modulation can then be achieved at gigahertz frequencies without suffering from the restriction in reduced emission area and small unit cell geometry. Such an arrangement has been designated photon assisted field emission device (PAFED).[7] Bypassing gate modulation has many advantages in addition to circumventing the capacitance limitation and reducing the risk of arc damage: increased emission area due to bypassing the capacitance limitations on gate modulation results in a reduced tip load, tailored harmonics in the power tube, ease of thermal management enabled by forced convection cooling, and the ability to combine various integrated devices with the PAFED.

Significant field emission current is triggered when the backside of the PAFED is illuminated by a light emitting diode or laser diode. A high resistivity semiconductor such as Si, whose conductivity and the quasi-Fermi level can be changed through the photoconductive effect, in which absorbed photons excite electrons from the valence band to the conduction band, is utilized. The increase in electron density in the conduction band of the Si field emitter tip will locally change the electron density, thereby causing the tip to change from its previous nonemitting condition to an electron emission condition. The dc biased electric field, combined with electron diffusion, will promote the drift of the excited electrons toward the field emitter tips.[7]

The standard method for evaluating field emission current from a metal[8] involves evaluating the transmission coefficient $T(k)$ and integrating it with the product of the supply function of electrons $f_0(k)[\#/\text{Å}^2]$ and the electron velocity $v(k)=\hbar k/m$ (Å/fs). The barrier height is typically the sum of the work function Φ [eV] and chemical potential μ [eV]. Image charge modifications, due to many-body exchange-correlation potentials,[9] lowers the barrier by $\sqrt{(4QF)}$, where F is the applied field [eV/Å] and $Q=\alpha_{\text{fs}}\hbar c(K_s-1)/4(K_s+1)\approx 3.6\,\text{eV Å}$ for metals, where the dielectric term $K_s \gg 1$, and α_{fs} is the fine structure constant.

[a]Author to whom correspondence should be addressed; electronic mail: kevin.jensen@nrl.navy.mil
[b]Also with: Department of Nuclear Engineering and Radiation Science, University of Michigan, Ann Arbor, MI 48109-2104.

$\ln(T(k))$ is assumed to be linear in energy with the Taylor expansion point taken as μ. Integrating the resulting $T(k)$ with the supply function $f_0(k)$ and velocity $v(k)=\hbar k/m$ results in the Fowler–Nordheim equation for current density.

For metals, the chemical potential μ is approximated by $\mu_0=(\hbar^2/2m)[3\pi^2/\rho]^{2/3}$ where $\mu_0=\mu(T=0\,\mathrm{K})$, and where ρ is the density of electrons (#/Å^3). The electron density in bulk semiconductors is orders of magnitude smaller than metals, indicating that the chemical potential must be treated more carefully because applied electric fields are not shielded as effectively (band bending). The Fowler–Nordheim equation requires a critical reexamination as follows. The electron density in a semiconductor can be calculated from[10] $\rho(x)=(2N_c/\sqrt{\pi})F_{1/2}(\beta\mu(x))$, where $N_c=M_c(m/2\pi\beta\hbar^2)^{3/2}$, $M_c=6$ for Si, $\mu(x)=\mu_0+\varphi(x)$, where φ is the solution to Poisson's equation, $F_{1/2}(x)$ is the Fermi–Dirac integral, and $\beta=1/k_BT$. For silicon, transverse t and parallel l effective masses combine so that $m=(m_l m_t^2)^{1/3}\approx 0.328\,m_0$, where $m_0=0.511\,\mathrm{MeV/c^2}$. For field emission conditions, the following approximation has been found to relate the externally applied field to the electrochemical potential at the surface:

$$F^2=\frac{4N_cK_s}{\sqrt{\pi}\beta}\int_0^\infty \sqrt{y}\ln(1+e^{\beta\mu-y})dy \approx 4N_cK_s\left(\frac{\beta\mu}{\pi}\right)^{1/2}\left(\frac{4}{15}\beta^2\mu^2+\frac{1}{6}\pi^2\right). \quad (1)$$

Equation (1) is solved iteratively to obtain $\mu(x)$ as a function of F and T.

Wigner distribution function simulations have shown that at fields where emission is significant, the zero emitted current approximation (ZECA) used to calculate $T(k)$ overestimates the band bending and therefore current density. The density profile presumed by ZECA is not valid near the vacuum interface.[11] Self-consistent calculations show, however, that a shifted image charge potential is valid.[12] The exchange-correlation potentials due to electron statistics and density variation, which cause deviations from the simple image charge form, may be approximated by[13]

$$V(x)=\mu+\Phi_0+\frac{8}{3\pi}Qk_F^3x_i^2-F(x-x_0)-\frac{Q}{(x+x_0)}, \quad (2)$$

where $x_0=\hbar/\sqrt{(2mV_{\max})}$, $V_{\max}$ is the maximum value of the potential $\hbar k_F=\sqrt{(2m\mu)}$, and $x_i(k_Fx_0)$ is the origin of the background positive charge. Because x_0 depends on F, it must be evaluated iteratively. Φ_0 is related to the experimental Φ by the relation $V(\infty)|_{F=0}=\Phi$. The *effective* work function Φ^* is defined as

$$\Phi^*=\Phi_0+\frac{8}{3\pi}Qk_F^3x_i^2+2Fx_0. \quad (3)$$

$V(x)$ is then well approximated by $\mu+\Phi^*-F(x+x_0)-Q/(x+x_0)$, i.e., a *shifted* image charge potential. Because x_0 and x_i depend on the maximum of $V(x)$, Eqs. (2)–(3) must be iteratively solved before Φ^* may be used in the Wentzel–Kramers–Brillouin analysis.

The choice of $E(k)\approx\mu$ is a poor expansion point for linearizing $\ln(T(k))$ when $\beta\mu$ is small. Performing the expansion about the maximum of the current integrand gives much greater accuracy, but must be iteratively and numerically sought. Comparisons were made with a recently developed exact (but more intensive) method of evaluating $T(k)$ using an Airy function approach, for which current estimates are shown to agree to within a factor of 2; such a method is sufficiently rapid on a desktop computer, and will therefore be used to find the current.

The ''statistical hyperbolic model'' of a field emitter[2,14] estimates tip and array current based on FEA geometrical and material parameters. The ratio of the array current to the product of the tip current with the number of tips defines the statistical factor Σ (which accounts for nonuniformity of emission, or the fact that current from tip to tip varies for a typical array). Departing from previous work, in addition to assuming a linear distribution in tip radii between the values a_s and $a_s(1+\Delta s)$, a linear distribution in effective work function Φ between the values Φ and $\Phi+\Delta\Phi$ is also assumed. The statistical factor becomes

$$\Sigma(V_g,\Delta s,\Delta\Phi)=\left(\frac{1-\exp(-b_a\Delta s)}{b_a\Delta s}\right)\times\left(\frac{1-\exp(-b_\phi\Delta\Phi)}{b_\phi\Delta\Phi}\right), \quad (5)$$

where b_a and b_ϕ are perforce numerically calculated using an Euler differencing scheme to approximate the derivatives $b_x=-\partial_s\ln(I_{\mathrm{tip}}(X))$, where X is either the tip radius a_s or the work function Φ. The semiconductor statistical hyperbolic model (SSHM) was validated by comparing predictions to silicon emitters manufactured by MCNC with the following parameters (not adjustable) obtained from the literature:[15] tip radius $a_s=30$ Å, gate radius $a_g=0.9\,\mu$m, hyperbolic cone half angle$=22°$, and number of tips$=18\,291$. All other parameters not specified are assumed to be typical of silicon. The parameters Δs and $\Delta\Phi$ were taken as $\Delta\Phi\approx 0.3$ eV (work function change for a generic adsorbate) and $\Delta s\approx 0.3$ (a ''common'' value, though it may be adjusted to achieve a better fit to experiment). For these parameters, Eq. (5) predicts 15%–20% of the tips contribute to the array current. In the experimental data of Ref. 15, a 100 kΩ gate resistor protected against arc damage (other resistances not considered here appear in the equivalent circuit model due to anode and base). Current intercepted by the gate is typically less than 0.5% for low gate voltages, but calculation shows that at 75 V, the anode current is a nontrivial fraction of the Child's law limit. If the current deflected to the gate increases to 1.5% of $I_{\mathrm{anode}}(\approx 4.5\,\mathrm{mA})$, which is reasonable,[16] then the gate voltage the tip experiences is 6.7 V smaller or, in terms of resistance, $R=\Delta V_{\mathrm{gate}}/I_{\mathrm{anode}}\approx 1500\,\Omega$. This effective resistance is incorporated into the voltage axis of Fig. 1. The model then agrees with published data. SSHM is therefore deemed sufficient to make estimates of PAFED performance.

Electron mobility values in silicon at room temperature are approximately 2000 cm^2/V s,[17] implying that the average time between collisions is around 370 fs. For an electron of effective mass m and a kinetic energy of 0.356 eV, the distance traveled in that time is approximately $d_r=0.23\,\mu$m (smaller if the electron velocity is closer to the thermal velocity, larger if field penetration occurs). Electrons created by

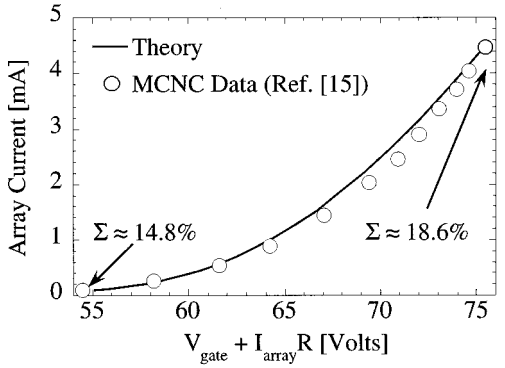

FIG. 1. Comparison of SSHM theory with MCNC data (Ref. 15).

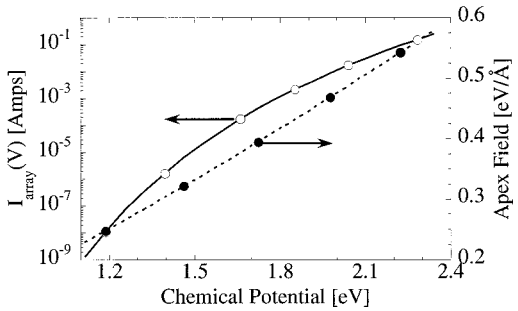

FIG. 2. Tip field and array current as a function of chemical potential according to SSHM theory.

a laser pulse on the backside of the field emitter will therefore potentially travel to the apex sufficiently fast to allow optical modulation at 10 GHz. Assuming *ad hoc* but nevertheless typical values for quantum efficiency (0.76), wavelength (8400 Å for $E=1.476\,\mathrm{eV}$), exposure area radius ($R=0.75\,\mu\mathrm{m}$), we find a $P=1\,\mathrm{MW/cm^2}$ laser will generate $N_l=5\,679\,219$ electrons in a $\delta t=0.1$ ns pulse with an energy above the conduction band in bulk of $E-E_g=0.356\,\mathrm{eV}$, where $E_g=1.12\,\mathrm{eV}$ is the band gap of silicon. A conservative estimate of the density increase is to assume that the electrons are uniformly distributed in a cone of half angle β_c and a height of d_t (the actual increase should be larger due to crowding as electrons approach the apex). For the parameters quoted, $\delta\rho\approx 0.002\,711\#/\mathrm{Å}^3$. The rise in the chemical potential due to the laser pulse becomes $\mu'=\mu[1+(\delta\rho/\rho)]^{2/3}$, where unprimed values are in the absence of the laser pulse.

In Fig. 2, the relationship between the array current and the chemical potential is shown for an emission disk of radius 1 mm with tips on a triangular lattice spaced 10 μm apart ($N_{\mathrm{tips}}=72\,552$). If the gate potential is held such that prior to the pulse the emission current is $0.1\,\mathrm{mA}(\mu=1.62\,\mathrm{eV})$, then our conservative estimate indicates that the pulse will cause μ to increase 16.5% and hence the current to increase by a factor of 23. Greater increasess may be achieved by more intense lasers in combination with operating at lower ''turn on'' gate voltages, but as shown by Whaley *et al.*,[4] the ratio $I_{\mathrm{ave}}/I_{\mathrm{peak}}$ does not have to be small to achieve good efficiency in an emission-gated TWT. Consequently, the capabilities implied by PAFED technology have significant promise.

We have provided a description of the operation of a PAFED. While our example focuses on the most demaning application of TWTs, this class of optically controlled electron emission devices clearly has a potentially wide range of applications. A model of field emission from silicon was developed, which accounts for complications due to band bending and departures from standard models used to estimate current from semiconductors. The model was validated against exact solutions to Schrödinger's equation, and the SSHM compared favorably to experimental data from MCNC. Current pulses over an order of magnitude greater than the base-line current could be obtained for generic parameters, demonstrating PAFED's utility for emission-gated devices.

The authors thank Dr. D. Temple of MCNC for permission to reproduce her data (Ref. 15).

[1] A. S. Gilmour, Jr., *Microwave Tubes* (Artech House, Norwood, MA, 1986).
[2] K. L. Jensen, Phys. Plasmas **6**, 2241 (1999).
[3] M. A. Kodis, K. L. Jensen, E. G. Zaidman, B. Goplen, and D. N. Smithe, IEEE Trans. Plasma Sci. **24**, 970 (1996).
[4] D. R. Whaley, B. Gannon, C. R. Smith, C. M. Armstrong, and C. A. Spindt, IEEE Trans. Plasma Sci. (accepted June 2000).
[5] K. L. Jensen, R. H. Abrams, and R. K. Parker, J. Vac. Sci. Technol. B **16**, 749 (1998).
[6] Photo-induced field emission has a mature history; recent examples: M. J. Hagmann, J. Vac. Sci. Technol. B **13**, 403 (1995); M. Takai, N. Suzuki, H. Morimoto, A. Hosono, and S. Kawabuchi, *ibid.* **16**, 780 (1998); For electron bunches generated by a laser pulse on a photocathode, see: F. V. Hartemann, S. N. Fochs, J. D. Mcnally, S. Burns, N. C. Luhmann, M. D. Perry, and K. R. Chu, Appl. Phys. Lett. **65**, 2404 (1994).
[7] D. S. McGregor, Y. Y. Lau, and K. L. Jensen, ''PAFED Driven RF Amplifier,'' Provisional Patent Application (January 12, 2000).
[8] A. Modinos, *Field, Thermionic, and Secondary Electron Spectroscopy* (Plenum, New York, 1984).
[9] A. Kiejna and K. F. Wojciechowski, *Metal Surface Electron Physics* (Pergamon, Oxford, 1996).
[10] S. M. Sze, *Physics of Semiconductor Devices*, 2nd ed. (Wiley, New York, 1981).
[11] K. L. Jensen, J. Vac. Sci. Technol. B **13**, 505 (1995).
[12] N. D. Lang and W. Kohn, Phys. Rev. B **7**, 3541 (1973).
[13] K. L. Jensen, J. Appl. Phys. **85**, 2667 (1999).
[14] K. L. Jensen, P. Mukhopadhyay-Phillips, E. G. Zaidman, K. Nguyen, M. A. Kodis, L. Malsawma, and C. Hor, Appl. Surf. Sci. **111**, 204 (1997).
[15] D. Temple, W. D. Palmer, L. N. Yadon, J. E. Mancusi, D. Vellenga, and G. E. McGuire, J. Vac. Sci. Technol. A **16**, 1980 (1998), a_s and β_c were extrapolated from Fig. 4. a_g and N were taken from the text and from Figure 9. The MCNC $I(V)$ data were interpolated from Fig. 9.
[16] K. L. Jensen, M. A. Kodis, R. A. Murphy, and E. G. Zaidman, J. Appl. Phys. **82**, 845 (1997).
[17] B. K. Ridly, *Quantum Processes in Semiconductors*, 2nd ed. (Oxford University Press, New York, 1988), See p. 129, Figure 3.21.